hydrous $Na[S_2CNMe_2]$ to $[WOCl_2(PMe_3)_3]$ gave $[WO(PMe_3)(S_2CNMe_2)_2]$ (**12**).[38] The temperature dependence of the dynamic ^1H NMR spectra of **12** has been interpreted in terms of a fluxional process (possibly involving rupture of a W–S bond), which equilibrates the inequivalent ligands in a structure with a cis orientation of the oxo and phosphine ligands—the appearance of four distinct benzylic resonances in ^{13}C spectra of **7** suggests a similar low-symmetry structure (Scheme III), but we see no comparable evidence for a low-energy fluxional rearrangement of **7**. The low symmetry within **7** was further confirmed by the observation in ^1H NMR spectra of a complex (18 resolved lines) resonance for the phosphine methylenes—this was closely simulated by PANIC[11] on the assumption that the methylene hydrogens are diastereotopic (see Experimental Section for parameters).

While this work was being prepared for publication, we were informed that Yu and Holm had independently discovered that $[WO_2(S_2CNR_2)_2]$ ($R_2 = Me_2, (CH_2)_5$) can be reduced to W(V) oxo-bridged dimers $[\{WO(S_2CNR_2)_2\}_2O]$ by $P(OMe)_3$,[39] from which they inferred the intermediate formation of the W(IV) oxo species $[WO(S_2CNR_2)_2]$. Our preparation of **7** remains the only case in which oxo atom transfer is used to reduce a $W^{VI}O_2$ complex to an isolated $W^{IV}O$ complex, and since a trialkylphosphine would be expected to be a somewhat less powerful oxo acceptor than a trialkyl phosphite (ca 13 kcal mol^{-1} from the data in Table V of ref 18), the success of reduction with PEt_3 suggests that oxo transfer from $W^{VI}O_2$ complexes may be less difficult than had been assumed.

It is notable that we have only been able to isolate a PEt_3 adduct of $[WO\{S_2CN(CH_2Ph)_2\}_2]$ (**11**)—attempts to limit the reduction of **6** to the production of **11** by using 1 equiv of PEt_3 have not led to tractable products, and we suspect that, in sharp contrast to the analogous molybdenum complexes, W(IV) oxo complexes $[WO(S_2CNR_2)_2]$ are only stable as adducts of donor ligands.

Conclusions

Photochemical. The sensitivity of $[(MoO\{S_2CN(CH_2Ph)_2\}_2)_2O]$ (**4**) and of $[(WO\{S_2CN(CH_2Ph)_2\}_2)_2O]$ (**5**) to ambient lighting is most reasonably interpreted in terms of facile photodisproportionation into the $M^{IV}O$ and $M^{VI}O_2$ complexes **8** plus **9** and **6** plus **11**, respectively, and the photoacceleration of the oxidation of **5** supports this suggestion. In conjunction with our previous observation of photodisproportionation of **1**$^{2+}$[4] and Richman's demonstration of photodisproportionation of $[\{Fe(TPP)\}_2O]$,[5] these results imply that photodisproportionation is probably a general reaction of complexes with a linear oxo bridge between two metal centers with odd (d^1–d^1 and d^5–d^5 in the cases above) electron centers.

We have not yet carried out detailed photophysical studies of **4** or **5**, and these will be experimentally challenging in both cases for a variety of reasons—the facility of the equilibrium thermal disproportionation of **4** precludes simple classical quantum yield studies and trapping experiments, while the limited solubility of **5** and the apparent inaccessibility by independent synthesis of the $W^{IV}O$ product **11** restricts photophysical studies of disproportionation of **5**. Until such studies have been completed, detailed speculation on the mechanism of the photodisproportionation is inappropriate, but it is certainly possible that it occurs from a distorted charge-transfer excited state as established by Richman for the $[\{Fe(TPP)\}_2O]$ case.[5b] It is interesting that the photoacceleration of the oxidation of **5** can be carried out by using long wavelength ($\lambda > 515$ nm) light, since this would indicate that the intense visible absorption at 517 nm, which must have charge-transfer character, is photoactive.

Synthetic. Controlled oxidation of $[W(CO)_3\{S_2CN(CH_2Ph)_2\}_2]$ (**10**) allows access to the W(VI) dioxo complex $[WO_2\{S_2CN(CH_2Ph)_2\}_2]$ (**6**) or the d^1–d^1 dimer $[(WO\{S_2CN(CH_2Ph)_2\}_2)_2O]$ (**5**). Reduction of **6** with PEt_3 leads to $[WO(PEt_3)\{S_2CN(CH_2Ph)_2\}_2]$ (**7**), a PEt_3 adduct of the $W^{IV}O$ complex, which would be the expected product of oxygen atom transfer from **6** to PEt_3—this is the first example in which reaction of a W(VI) dioxo complex with an oxygen atom acceptor has been observed to give an isolable W(IV) oxo complex.

Acknowledgment. This work was supported in part by the Office of Naval Research. We thank Professor R. H. Holm for prepublication communication of the information in ref 18.

Supplementary Material Available: Tables of full crystal data, anisotropic temperature factors, and hydrogen atom coordinates for $[(WO\{S_2CN(CH_2Ph)_2\}_2)_2O]$ (3 pages); a listing of calculated and observed structure factors (22 pages). Ordering information is given on any current masthead page.

---

[38] Carmona, E.; Sachez, L.; Poveda, M. L.; Jones, R. A.; Hefner, J. G. *Polyhedron* **1983**, *2*, 797.

[39] Holm, R. H. Personal communication. Details of this work have been published.[18]

Contribution from the Institut für Anorganische und Analytische Chemie
der Freien Universität Berlin, Fabeckstrasse 34-36, D-1000 Berlin 33, FRG

Regioselective Coupling of a Fluoromethylidyne Ligand of Nonacarbonylbis(μ_3-fluoromethylidyne)triiron with Alkynes

Dieter Lentz* and Heike Michael-Schulz

Received December 11, 1989

Nonacarbonylbis(μ_3-fluoromethylidyne)triiron, $Fe_3(CO)_9(\mu_3\text{-}CF)_2$ (**1**), reacts with alkynes $H{-}C{\equiv}C{-}R$ (**2a–f**), forming diferra–allyl clusters $Fe_3(CO)_8(\mu_3\text{-}CF)(\mu_3\text{-}CF{-}CH{-}CR)$ (**3a–f**). According to the spectroscopic data of the products **3a–f**, the carbon–carbon bond formation occurs selectively at the sterically less hindered site of the alkyne. The structure of $Fe_3(CO)_8(\mu_3\text{-}CF)(\mu_3\text{-}CF{-}CH{-}C{-}O{-}C_2H_5)$ (**3c**) has been established by an X-ray crystal structure determination, monoclinic, $P2_1/c$, $a = 15.396$ (4) Å, $b = 8.153$ (4), $c = 14.915$ (3) Å, $\beta = 103.24$ (6)°. With the alkynes $H_3C{-}C{\equiv}C{-}R$ (**2g–l**), the regioselectivity of the carbon–carbon bond formation is less distinct. The clusters $Fe_3(CO)_8(\mu_3\text{-}CF)[\mu_3\text{-}CF{-}C(CH_3){-}CR]$ (**3(I)g–l**) and the isomers $Fe_3(CO)_8(\mu_3\text{-}CF)(\mu_3\text{-}CF{-}CR{-}CCH_3)$ (**3(II)g–l**) are obtained. The ratio of the isomers strongly depends on the steric demand and the electronic effects of the substituent R.

Introduction

In contrast to the well-established chemistry of the nonacarbonyl(μ_3-alkylidyne)tricobalt clusters[1] and their derivatives obtained by metal-exchange reactions,[2] only a few nonacarbonylbis(μ_3-alkylidyne)triiron clusters $Fe_3(CO)_9(\mu_3\text{-}CCH_3)(C{-}OCH_3)$,[3] $Fe_3(CO)_9(\mu_3\text{-}CF)_2$,[4] $Fe_3(CO)_9(\mu_3\text{-}C{-}CH_3)(\mu_3\text{-}C{-}$

---

[1] Kemmitt, R. D. W.; Russel, D. R. In *Comprehensive Organometallic Chemistry*; Wilkinson, G., Ed.; Pergamon: Oxford, England, 1982; Vol. 5. Penfold, B. R.; Robinson, B. H. *Acc. Chem. Res.* **1973**, *6*, 73. Seyferth, D. *Adv. Organomet. Chem.* **1976**, *14*, 97.

[2] Beurich, H.; Vahrenkamp, H. *Chem. Ber.* **1982**, *115*, 2385. Beurich, H.; Blumhofer, R.; Vahrenkamp, H. *Chem. Ber.* **1982**, *115*, 2409.

[3] Wong, W.-K.; Chiu, K. W.; Wilkinson, G.; Galas, A. M.-R.; Thornton-Pett, M.; Hursthouse, M. B. *J. Chem. Soc., Dalton Trans.* **1983**, 1557.

$OC_2H_5)$,[5] $Fe_3(CO)_9(\mu_3\text{-}CH)(\mu_3\text{-}C{-}O{-}CH_3)$,[6] $Fe_3(CO)_9(\mu_3\text{-}CH)(\mu_3\text{-}C{-}N(CH_3)_2)$,[7] $Fe_3(CO)_9(\mu_3\text{-}CR)(\mu_3\text{-}CR')$,[8] $Fe_3(CO)_9(\mu_3\text{-}C{-}O{-}CH_3)_2$,[9] $Fe_3(CO)_9(\mu_3\text{-}CCl)_2$,[10] $Fe_3(CO)_9(\mu_3\text{-}CBr)(\mu_3\text{-}CCOOR)$,[10] and $Fe_3(CO)_6(\eta^6\text{-}C_6H_6)(\mu_3\text{-}CCl)(\mu_3\text{-}C{-}COOEt)$[10] have been recently synthesized. Mathieu et al. have studied the reactivity of $Fe_3(CO)_9(\mu_3\text{-}C{-}CH_3)(\mu_3\text{-}C{-}OC_2H_5)$ with alkynes and obtained ferrole type closo clusters.[5] Depending on the alkyne, they obtained several isomers. In the reaction of $Fe_3(CO)_9(\mu_3\text{-}CF)_2$ with various alkynes $R{-}C{\equiv}C{-}R$ no ferrole formation was observed.[11] Ferra–allyl clusters $Fe_3(CO)_8(\mu_3\text{-}CF)(\mu_3\text{-}CF{-}CR{-}CR)$, which possess a capped nido structure, were obtained as the only product. With the phosphaalkyne $t\text{-}C_4H_9{-}C{\equiv}P$, however, a ferraphosphacyclopentadiene ring was formed by carbon–carbon and carbon–phosphorus bond formation.[12] Only two further diferra–allyl clusters $(\eta^5\text{-}C_5H_2Et_3)Fe_3(CO)_7(\mu_3\text{-}CH{-}CH{-}CEt)$[13] and $HFe_3(CO)_9(\mu_3\text{-}CMe{-}CPh{-}CH)$[14] have been reported. There exist several dimetalla–allyl clusters of ruthenium and osmium;[15] some of them have been prepared by an alkylidyne–alkyne coupling reaction.[16] In continuation of our studies on the reactivity of nonacarbonylbis(μ_3-fluoromethylidyne)triiron, we have studied the reactions of $Fe_3(CO)_9(\mu_3\text{-}CF)_2$ with asymmetric alkynes $H{-}C{\equiv}C{-}R$ and $H_3C{-}C{\equiv}C{-}R$ in order to obtain information about the regioselectivity of the reactions.

Experimental Section

All reactions were carried out under dry argon by using standard Schlenk tube and vacuum techniques. Volatile alkynes were handled on a conventional vacuum line and amounts were determined by *PVT* techniques. Photolyses were carried out in a 100-mL or 250-mL Pyrex glass photoreactor using a high-pressure mercury lamp (Philips HPK 125 W). ^1H NMR, ^{19}F NMR, and ^{13}C NMR spectra were recorded by using a Jeol FX 90Q instrument using TMS, $CFCl_3$, and TMS or solvent signals as reference standards. The product composition and isomeric ratios were monitored by TLC chromatography and, directly after filtration of the reaction mixture over silica to remove paramagnetic decomposition products, by ^{19}F NMR spectroscopy. Computer simulations of the ABC_3 spectra were performed with the LAOCN3 program.[17] IR spectra were taken on a Perkin-Elmer 883 instrument. Mass spectra were obtained on a Varian MAT 711 spectrometer (80 eV). $Fe_3(CO)_9(\mu_3\text{-}CF)_2$[4] (**1**), $H{-}C{\equiv}C{-}CH_3$[18] (**2a**), $H{-}C{\equiv}C{-}O{-}C_2H_5$[19] (**2c**), $H{-}C{\equiv}C{-}CF_3$[20] (**2e**), $H{-}C{\equiv}C{-}SF_5$[21] (**2f**) $H_3C{-}C{\equiv}C{-}O{-}C_2H_5$[22] (**2i**), and $H_3C{-}C{\equiv}C{-}C(H)(CH_3)_2$[23] (**2h**) were prepared by literature methods. The other alkynes are commercially available and were used as received.

$Fe_3(CO)_8(\mu_3\text{-}CF)(\mu_3\text{-}CF{-}CH{-}CCH_3)$ (3a). $Fe_3(CO)_9(\mu_3\text{-}CF)_2$ (**1**) (110 mg, 0.23 mmol) was dissolved in 100 mL of *n*-hexane in a 100-mL photoreactor. The reactor was cooled with liquid nitrogen, and $HC{\equiv}CCH_3$ (**2a**) (7 mmol) was condensed onto the reaction mixture. The reaction mixture was then irradiated for 10 min at 15 °C. Most of the solvent was removed under vacuum, and the remaining solution was filtered through a layer of silica. After the solvent was removed under vacuum, the residue was dissolved in a minimum amount of *n*-pentane and recrystallized at −20 °C, yielding **3a** (54 mg, 47%) as green crystals, mp 108–109 °C. MS (80 eV) [*m/z* (%, assignment)]: 494 (17 M^+), 466 (48, $M^+ - CO$), 438 (24, $M^+ - 2CO$), 354 (39 $M^+ - 5CO$), 326 (81, $M^+ - 6CO$), 298 (48, $M^+ - 7CO$), 270 (80 $M^+ - 8CO$), and smaller fragment ions. High-resolution MS of the molecular ion: calc, *m/e* 493.7924; found, *m/e* 493.7922.

$Fe_3(CO)_8(\mu_3\text{-}CF)(\mu_3\text{-}CF{-}CH{-}CC_6H_5)$ (3b). $Fe_3(CO)_9(\mu_3\text{-}CF)_2$ (**1**) (200 mg, 0.42 mmol) and $HC{\equiv}CC_6H_5$ (**2b**) (46 μL, 0.42 mmol) were added to 100 mL of *n*-pentane. The reaction mixture was irradiated in a photoreactor for 25 min at 15 °C. The progress of the reaction was monitored by TLC (*n*-pentane). After complete reaction the solvent was removed under vacuum. The residue was dissolved in a minimum amount of CH_2Cl_2 followed by preparative TLC (*n*-pentane) and crystallization from *n*-pentane to give **3b** (109 mg, 47%) as green crystals, mp 120–121 °C. MS (80 V) [*m/e* (%, assignment)]: 556 (8, M^+), 528 (53, $M^+ - CO$), 500 (68, $M^+ - 2CO$), 472 (32, $M^+ - 3CO$), 444 (67, $M^+ - 4CO$), 416 (100, $M^+ - 5CO$), 388 (19, $M^+ - 6CO$), 360 (58, $M^+ - 7CO$), 332 (85, $M^+ - 8CO$), and smaller fragment ions. High-resolution MS of the molecular ion: calc, *m/e* 555.8084; found, 555.8079.

$Fe_3(CO)_8(\mu_3\text{-}CF)(\mu_3\text{-}CF{-}CH{-}COC_2H_5)$ (3c). $Fe_3(CO)_9(\mu_3\text{-}CF)_2$ (**1**) (291 mg, 0.6 mmol) and $HC{\equiv}COC_2H_5$ (**2c**) (120 mg, 1.8 mmol) were added to 100 mL of *n*-pentane. The solution was irradiated in a photoreactor for 80 min at 15 °C. The reaction mixture was then pumped to dryness followed by dissolution of the crude product in *n*-pentane and purification by column chromatography (silica, *n*-pentane). A violet fraction was recrystallized from *n*-pentane at −78 °C to give **3c** (81 mg, 26%) as dark green crystals, mp 119–120 °C. MS (80 eV) [*m/e* (%, assignment)]: 524 (37, M^+), 496 (49, $M^+ - CO$), 468 (37, $M^+ - 2CO$), 440 (37, $M^+ - 3CO$), 412 (96, $M^+ - 4CO$), 384 (63, $M^+ - 5CO$), 356 (50, M^+ 6CO), 328 (57, $M^+ - 7CO$), 300 (100, $M^+ - 8CO$). High-resolution MS of the molecular ion: calc, *m/e* 523.8028; found, *m/e* 523.8020.

$Fe_3(CO)_8(\mu_3\text{-}CF)[\mu_3\text{-}CF{-}CH{-}CSi(CH_3)_3]$ (3d). $Fe_3(CO)_9(\mu_3\text{-}CF)_2$ (**1**) (284 mg, 0.59 mmol) and $HC{\equiv}CSi(CH_3)_3$ (**2d**) (120 mg, 1.2 mmol) were added to 100 mL of *n*-pentane and irradiated in a photoreactor for 10 min. After complete reaction (TLC, *n*-pentane) the reaction mixture was filtered through a layer of silica (*n*-pentane), and the solvent was removed under vacuum. Crystallization from *n*-pentane at −78 °C gave **3d** (195 mg, 59%) as dark green crystals, mp 57–58 °C. MS (80 eV) [*m/e* (%, assignment)]: 552 (1, M^+), 524 (8, $M^+ - CO$), 496 (4, $M^+ - 2CO$), 468 (8, $M^+ - 3CO$), 440 (49, $M^+ - 4CO$), 412 (41, $M^+ - 5CO$), 384 (57, $M^+ - 6CO$), 356 (39, $M^+ - 7CO$), 328 (100, $M^+ - 8CO$). High-resolution MS of the molecular ion: calc, *m/e* 551.8161; found, *m/e* 551.8168.

$Fe_3(CO)_8(\mu_3\text{-}CF)(\mu_3\text{-}CF{-}CH{-}CCF_3)$ (3e). $Fe_3(CO)_9(\mu_3\text{-}CF)_2$ (**1**) (300 mg, 0.63 mmol) was added to 100 mL of *n*-pentane in a photoreactor. The solution was cooled with liquid nitrogen, and $HC{\equiv}CCF_3$ (**2e**) (2 mmol) was condensed into the photoreactor. The reaction mixture was warmed to −60 °C and irradiated for 5 h. The solvent was removed under vacuum, and the residue was dissolved in a minimal

---

(4) Lentz, D.; Brüdgam, I.; Hartl, H. *Angew. Chem.* **1985**, *97*, 115; *Angew. Chem., Int. Ed. Engl.* **1985**, *24*, 119.

(5) Nuel, D.; Dahan, F.; Mathieu, R. *J. Am. Chem. Soc.* **1985**, *107*, 1658.

(6) Hriljac, J. A.; Shriver, D. F. *J. Am. Chem. Soc.* **1987**, *109*, 6010.

(7) Cabrera, E.; Daran, J. C.; Jeannin, Y. *J. Chem. Soc., Chem. Commun.* **1988**, 607.

(8) Nuel, D.; Mathieu, R. *Organometallics* **1988**, *7*, 16. Suades, J.; Dahan, F.; Mathieu, R. *Organometallics* **1988**, *7*, 47.

(9) Aradi, A. A.; Grevels, F.-W.; Krüger, C.; Raabe, E. *Organometallics* **1988**, *7*, 812.

(10) Lentz, D.; Michael, H. *Inorg. Chem.* **1989**, *28*, 3396.

(11) Lentz, D.; Michael. H. *Chem. Ber.* **1988**, *121*, 1413.

(12) Lentz, D.; Michael, H. *Angew. Chem.* **1989**, *101*, 330; *Angew. Chem., Int. Ed. Engl.* **1989**, *28*, 321.

(13) Sappa, E.; Tiripicchio, A.; Lanfredi, A. M. M. *J. Chem. Soc., Dalton Trans.* **1978**, 552.

(14) Nuel, D.; Mathieu, R. *Organometallics* **1988**, *4*, 16.

(15) Cox, A.; Woodward, P. *J. Chem. Soc. A* **1971**, 3599. Evans, M.; Hursthouse, M.; Randall, E. W.; Rosenberg, E.; Milone, L.; Valle, M. *J. Chem. Soc., Chem. Commun.* **1972**, 545. Bruce, M. I.; Cairns, M. A.; Green, M. *J. Chem. Soc., Dalton Trans.* **1972**, 1293. Gambino, O.; Valle, M.; Aime, S.; Vaglio, G. A. *Inorg. Chim. Acta* **1974**, *8*, 71. Aime, S.; Jannon, G.; Osella, D.; Deeming, A. J. *J. Organomet. Chem.* **1981**, *214*, C15. Humphries, A. P.; Knox, S. A. R. *J. Chem. Soc., Dalton Trans.* **1975**, 1710. Castiglioni, M.; Milone, L.; Osella, D.; Vaglio, G. A.; Valle, M. *Inorg. Chem.* **1976**, *15*, 394. Aime, S.; Osella, D.; Arce, A. J.; Deeming, A. J.; Hursthouse, M. B.; Galas, A. M. R. *J. Chem. Soc., Dalton Trans.* **1984**, 1981. Aime, S.; Jannon, G.; Osella, D.; Arce, A. J.; Deeming, A. J. *J. Chem. Soc., Dalton Trans.* **1984**, 1987. Deeming, A. J.; Hasso, S.; Underhill, M. *J. Chem. Soc., Dalton Trans.* **1975**, 1614. Hanson, B. E.; Johnson, B. F. G.; Lewis, J.; Raithby, P. R. *J. Chem. Soc., Dalton Trans.* **1980**, 1852. Skinner, D. M.; Rosenberg, E.; Brackner-Novak, J.; Aime, S.; Osella, D.; Gobetto, R.; Milone, L. *Organometallics* **1988**, *7*, 856.

(16) (a) Beanan, L. B.; Rahman, Z. A.; Keister, J. B. *Organometallics* **1983**, *2*, 1062. Beanan, L. R.; Keister, J. B. *Organometallics* **1985**, *4*, 1713. (b) Churchill, M. R.; Ziller, J. W.; Shapley, J. R.; Yeh, W.-Y. *J. Organomet. Chem.* **1988**, *353*, 103.

(17) Bothner-By, A. A.; Castellano, S. M. LAOCN3 (A Program for Computer Simulation of Complex NMR Spectra. In *Computer Programs for Chemistry*; de Tar, D. F., Ed.; W. A. Benjamin, Inc.: New York, 1968; Vol. 1, Chapter 3. Clark, M.; Thrasher, J. S. MS-DOS Version for IBM Personal Computer. The University of Alabama, Tuscaloosa, AL.

(18) Hurd, C. D.; Meinert, R. N.; Spence, L. U. *J. Am. Chem. Soc.* **1930**, *52*, 1138.

(19) Jones, E. R. H.; Eglinton, G.; Whiting, M. C.; Shaw, B. L. *Organic Syntheses*; Wiley: New York, 1963; Collect. Vol. IV, p 404.

(20) Finnegan, W. G.; Norris, W. P. *J. Org. Chem.* **1963**, *28*, 1139.

(21) Wessel, J.; Kleemann, G.; Seppelt, K. *Chem. Ber.* **1983**, *116*, 2399.

(22) Miller, H. N.; Greenlee, K. W.; Drefer, J. M.; Board, C. E. *J. Org. Chem.* **1954**, *19*, 1882.

(23) Alkema, H. J.; Ahrens, J. F. *Recl. Trav. Chim. Pays-Bas* **1960**, *79*, 1257.

amount of dichloromethane. Purification by column chromatography (silica, *n*-pentane) gave a green main fraction, which was eluated first. Removal of solvent and crystallization from *n*-pentane gave **3e** (130 mg, 38%) as green crystals, mp 99–100 °C. MS (80 eV) [*m/e* (%, assignment)]: 548 (18, M^+), 520 (40, $M^+ - CO$), 492 (9, $M^+ - 2CO$), 464 (20, $M^+ - 3CO$), 436 (15, $M^+ - 4CO$), 408 (33, $M^+ - 5CO$), 380 (69, $M^+ - 6CO$), 352 (14, $M^+ - 7CO$), 324 (59, $M^+ - 8CO$). High-resolution MS of the molecular ion: calc, *m/e* 547.7639; found, *m/e* 547.7639.

$Fe_3(CO)_8(\mu_3\text{-}CF)(\mu_3\text{-}CF\text{–}CH\text{–}CSF_5)$ (3f). A photoreactor with a solution of $Fe_3(CO)_9(\mu_3\text{-}CF)_2$ (**1**) (200 mg, 0.42 mmol) in 100 mL of *n*-pentane was cooled with liquid nitrogen, and $HC{\equiv}CSF_5$ (**2f**) (0.7 mmol) was condensed into the photoreactor. The solution was warmed to 0 °C and irradiated for 4 h. The solvent was removed under vacuum, and the residue was dissolved in a minimum amount of CH_2Cl_2. Purification by column chromatography (silica, *n*-pentane) and crystallization from *n*-pentane at −78 °C gave **3f** (38 mg, 14%) as green crystals, mp 87–89 °C. MS (80 eV) [*m/e* (%, assignment)]: 578 (21, $M^+ - CO$), 550 (5, $M^+ - 2CO$), 442 (14, $M^+ - 2CO - SF_4$), 414 (10, $M^+ - 3CO - SF_4$), 386 (15, $M^+ - 4CO - SF_4$), 358 (24, $M^+ - 5CO - SF_4$), 330 (48, $M^+ - 6CO$), 302 (79, $M^+ - 7CO - SF_4$), 274 (52, $M^+ - 8CO - SF_4$), and smaller fragment ions. High-resolution MS of the ion $M^+ - CO$: calc, *m/e* 577.7377; found, *m/e* 577.7379.

$Fe_3(CO)_8(\mu_3\text{-}CF)(\mu_3\text{-}CF\text{–}CCH_3\text{–}CC_2H_5)$ (3(I)g) and $Fe_3(CO)_8(\mu_3\text{-}CF)(\mu_3\text{-}CF\text{–}CC_2H_5\text{–}CCH_3)$ (3(II)g). $Fe_3(CO)_9(\mu_3\text{-}CF)_2$ (**1**) (200 mg, 0.42 mmol) and $CH_3\text{–}C{\equiv}C\text{–}C_2H_5$ (**2g**) (60 μL, 0.6 mmol) were dissolved in 100 mL of *n*-pentane. The solvent was removed under vacuum, and the residue was dissolved in a minimum of CH_2Cl_2 and filtered through a layer of silica by using *n*-pentane as an eluent. Removal of the solvent under vacuum gave **3g** (111 mg, 50.6 %) as a green waxy material, which according to the NMR spectra consists of a mixture of the two isomers **3(I)g** and **3(II)g**. MS (80 eV) [*m/e* (%, assignment)]: 522 (9, M^+), 494 (39, $M^+ - CO$), 466 (20, $M^+ - 2CO$), 438 (11, $M^+ - 3CO$), 410 (30, $M^+ - 4CO$), 382 (44, $M^+ - 5CO$), 354 (100, $M^+ - 6CO$), 326 (71, $M^+ - 7CO$), 298 (68, $M^+ - 8CO$), and smaller fragment ions. High-resolution MS of the molecular ion: calc, *m/e* 521.9697; found, *m/e* 521.8230.

$Fe_3(CO)_8(\mu_3\text{-}CF)[\mu_3\text{-}CF\text{–}C(CH_3)\text{–}CCH(CH_3)_2]$ (3(I)h) and $Fe_3(CO)_8(\mu_3\text{-}CF)[\mu_3\text{-}CF\text{–}CCH(CH_3)_2\text{–}CCH_3]$ (3(II)h). $Fe_3(CO)_9(\mu_3\text{-}CF)_2$ (**1**) (180 mg, 0.38 mmol) and $CH_3C{\equiv}CCH(CH_3)_2$ (**2h**) (50 μL, 0.5 mmol) were added to 100 mL of *n*-pentane. The solution was irradiated for 25 min in a photoreactor. Most of the solvent was removed under vacuum, and the remaining solution was filtered over silica. The solvent of the green solution was removed under vacuum, and the residue was dried in vacuum. **3i** (130 mg, 68%) was isolated as a green oily liquid, which contains both isomers in a ratio of about 2:1. MS (80 eV) [*m/e* (%, assignment)]: 536 (1, M^+), 508 (16, $M^+ - CO$), 480 (10, $M^+ - 2CO$), 452 (9, $M^+ - 3CO$), 424 (38, $M^+ - 4CO$), 396 (69, $M^+ - 5CO$), 368 (73, $M^+ - 6CO$), 340 (89, $M^+ - 7CO$), 312 (100, $M^+ - 8CO$), and smaller fragment ions. High-resolution MS of the molecular ion: calc, *m/e* 507.8442; found, *m/e* 507.8439.

$Fe_3(CO)_8(\mu_3\text{-}CF)(\mu_3\text{-}CF\text{–}CCH_3\text{–}COC_2H_5)$ (3(I)i). $Fe_3(CO)_9(\mu\text{-}CF)_2$ (**1**) (200 mg, 0.42 mmol) and $CH_3C{\equiv}COC_2H_5$ (**2i**) (58 mg, 0.84 mmol) were added to 100 mL of *n*-pentane. The solution was irradiated in a photoreactor for 20 min. Purification by preparative TLC (*n*-pentane) gave two fractions. Crystallization of the main fraction from *n*-pentane at −20 °C gave **3(I)i** (97 mg, 43%), mp 107–108 °C. MS (80 eV) [*m/e* (%, assignment)]: 538 (29, M^+), 510 (91, $M^+ - CO$), 482 (57, $M^+ - 2CO$), 454 (37, $M^+ - 3CO$), 426 (100, $M^+ - 4CO$), 398 (65, $M^+ - 5CO$), 370 (69, $M^+ - 6CO$), 342 (94, $M^+ - 7CO$), 314 (94, $M^+ - 8CO$), and smaller fragment ions. High-resolution MS of the molecular ion: calc, *m/e* 537.8186; found, *m/e* 537.8184.

$Fe_3(CO)_8(\mu_3\text{-}CF)(\mu_3\text{-}CF\text{–}CCH_3\text{–}CC_6H_5)$ (3(I)k). $Fe_3(CO)_9(\mu_3\text{-}CF)_2$ (**1**) (200 mg, 0.42 mmol) and $CH_3C{\equiv}CC_6H_5$ (**2k**) (100 mg, 0.84 mmol) were added to 100 mL of *n*-pentane. The solution was irradiated for 25 min in a photoreactor. The solvent was removed under vacuum. The residue was dissolved in a minimum amount of CH_2Cl_2, and the mixture was filtered through a layer of silica (*n*-pentane). Removal of solvent and crystallization from *n*-pentane at −78 °C gave **3(I)k** (94 mg, 40%) as dark green crystals, mp 106–107 °C. MS (80 eV) [*m/e* (%, assignment)]: 570 (8, M^+), 542 (50, $M^+ - CO$), 514 (67, $M^+ - 2CO$), 486 (29, $M^+ - 3CO$), 458 (59, $M^+ - 4CO$), 430 (79, $M^+ - 5CO$), 402 (17, $M^+ - 6CO$), 374 (57, $M^+ - 7CO$), 346 (60, $M^+ - 8CO$), and smaller fragment ions. High-resolution MS of the molecular ion: calc, *m/e* 569.8235; found, *m/e* 569.8235.

$Fe_3(CO)_8(\mu_3\text{-}CF)[\mu\text{-}CF\text{–}C(COOCH_3)\text{–}CCH_3)$ (3(II)l). $Fe_3(CO)_9(\mu_3\text{-}CF)_2$ (**1**) (100 mg, 0.2 mmol) and $CH_3\text{–}C{\equiv}COOCH_3$ (**2l**) (30 mg, 0.3 mmol) were added to 100 mL of *n*-pentane. The solution was irradiated for 25 min by using a photoreactor. The solvent was removed in vacuo. The residue was dissolved in a minimum of dichloromethane, and the mixture was filtered through a thin layer of silica by using *n*-pentane as an eluent. Removal of the solvent and crystallization from *n*-pentane at −78 °C gave **3(II)l** (46 mg, 42%) as dark green crystals, mp 94–95 °C. MS (80 eV) [*m/e* (%, assignment)]: 552 (19, M^+), 524 (59, $M^+ - CO$), 496 (34, $M^+ - 2CO$), 468 (19, $M^+ - 3CO$), 440 (18, $M^+ - 4CO$), 412 (47, $M^+ - 5CO$), 384 (52, $M^+ - 6CO$), 356 (100, $M^+ - 7CO$), 328 (77, $M^+ - 8CO$), and smaller fragment ions. High-resolution MS of the molecular ion: calc, *m/e* 551.7977; found, *m/e* 551.7989.

Scheme I

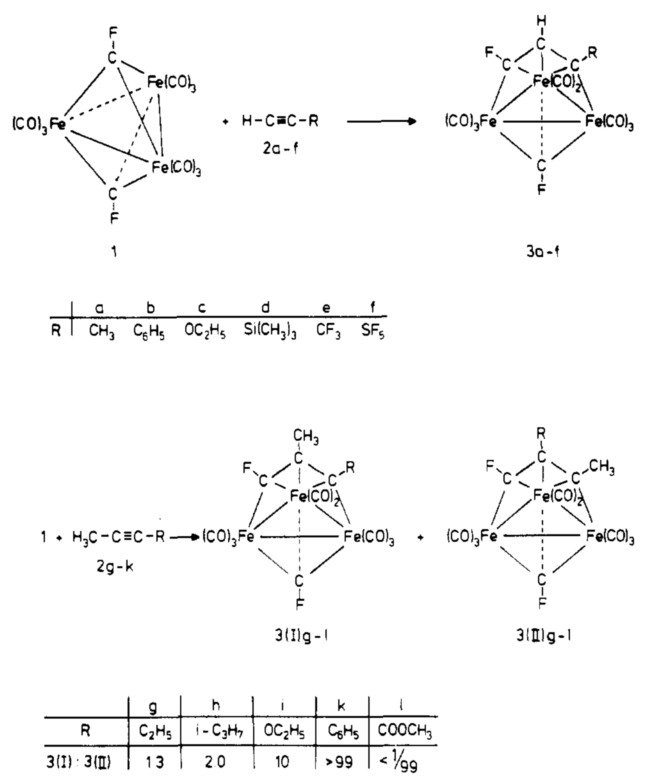

R	a	b	c	d	e	f
R	CH_3	C_6H_5	OC_2H_5	$Si(CH_3)_3$	CF_3	SF_5

	g	h	i	k	l
R	C_2H_5	i-C_3H_7	OC_2H_5	C_6H_5	$COOCH_3$
3(I) : 3(II)	1.3	2.0	10	>99	<1/99

Table I. Crystallographic Data for $Fe_3(CO)_8(\mu_3\text{-}CF)(\mu_3\text{-}CF\text{–}CH\text{–}COC_2H_5)$ (**3c**)

formula $C_{14}H_6F_2Fe_3O_9$	fw 523.8
a = 15.396 (4) Å	space group $P2_1/c$ (No. 14)
b = 8.153 (4) Å	λ = 0.71069 Å
c = 14.915 (3) Å	d_{calcd} = 1.92 g cm^{-3}
β = 103.24 (6) deg	μ(Mo Kα) = 25.0 cm^{-1}
V = 1822.4 Å$_3$	$R(F_o)$ = 0.032
Z = 4	

X-ray Crystal Structure Determination of $Fe_3(CO)_8(\mu_3\text{-}CF)(\mu_3\text{-}CF\text{–}CH\text{–}COC_2H_5)$ (3c). A suitable crystal (0.18 × 0.35 × 0.42 mm^3) of **3c**, obtained by slow cooling of a *n*-hexane solution, was sealed in a glass capillary. The data were collected by using a STOE diffractometer and reduced to structure factors by correction for Lorentz and polarization effects. The space group $P2_1/c$ (No. 14) was uniquely defined by systematic absences. A numerical absorption correction, ABSCOR,[24] was applied. The structure was solved by direct method, MULTAN.[25] Successive difference Fourier maps and least-squares refinement cycles, XRAY 76,[26] revealed the positions of all atoms. All non-hydrogen atoms were refined anisotropically. ORTEP[27] was used for molecular drawings.

Results

The reactions of this work are summarized in Scheme I. The infrared and ^1H, ^{19}F, and ^{13}C NMR spectroscopic data for the compounds **3a–l** are presented in Tables III and IV. An X-ray crystal structure determination was undertaken for $Fe_3(CO)_8(\mu_3\text{-}CF)(\mu_3\text{-}CF\text{–}CH\text{–}C\text{–}O\text{–}C_2H_5)$ (**3c**). The data are summarized in Table I. The final fractional atomic coordinates are listed in Table II. Important bond lengths and angles are summarized

---

(24) Burnham, C. W. *Am. Mineral.* **1966**, *51*, 159. Modified by W. Dreissig, Freie Universität Berlin.

(25) Germain, G.; Main, P.; Woolfson, M. M. *Acta Crystallogr., Sect. A* **1971**, *A27*, 368.

(26) Stewart, J. M. Program System for X-ray Crystallography. Computer Science Center, University of Maryland, 1976.

(27) Johnson, C. K. ORTEP II. Report ORNL-5138; Oak Ridge National Laboratory: Oak Ridge, TN, 1970.

Table II. Atomic Coordinates for Non-Hydrogen Atoms (Standard Deviations in Parentheses)

atom	*x*	*y*	*z*
Fe1	0.30014 (4)	−0.11573 (7)	0.80264 (4)
Fe2	0.18683 (3)	0.11011 (7)	0.77837 (4)
Fe3	0.35663 (4)	0.17170 (8)	0.83122 (4)
C1	0.2304 (3)	−0.2880 (6)	0.8070 (3)
C2	0.3960 (3)	−0.2284 (7)	0.8604 (3)
C3	0.1608 (3)	0.2594 (5)	0.6863 (3)
C4	0.1554 (3)	0.2399 (5)	0.8643 (3)
C5	0.0819 (3)	0.0031 (6)	0.7654 (3)
C6	0.3479 (3)	0.3083 (6)	0.9234 (3)
C7	0.3504 (3)	0.3340 (7)	0.7482 (3)
C8	0.4749 (3)	0.1538 (7)	0.8817 (3)
C9	0.2776 (3)	0.0246 (5)	0.8847 (3)
C10	0.3696 (3)	0.0241 (5)	0.7315 (3)
C11	0.3031 (3)	−0.0437 (6)	0.6631 (3)
C12	0.2170 (3)	−0.0353 (5)	0.6805 (3)
C13	0.1566 (4)	−0.2037 (8)	0.5474 (4)
C14	0.0672 (6)	−0.264 (1)	0.4996 (6)
O1	0.1846 (3)	−0.3961 (5)	0.8106 (3)
O2	0.4564 (3)	−0.2990 (6)	0.8989 (3)
O3	0.1442 (2)	0.3519 (4)	0.6280 (2)
O4	0.1341 (2)	0.3162 (4)	0.9193 (2)
O5	0.0158 (2)	−0.0621 (5)	0.7593 (3)
O6	0.3445 (3)	0.3959 (5)	0.9820 (3)
O7	0.3467 (3)	0.4370 (5)	0.6955 (3)
O8	0.5496 (2)	0.1447 (6)	0.9131 (3)
O9	0.1451 (2)	−0.1055 (4)	0.6245 (2)
F1	0.2711 (2)	0.0176 (2)	0.9736 (1)
F2	0.4537 (2)	−0.0031 (4)	0.7184 (2)

in Table V. The molecular structure and atom-numbering scheme are depicted in FIgure 1.

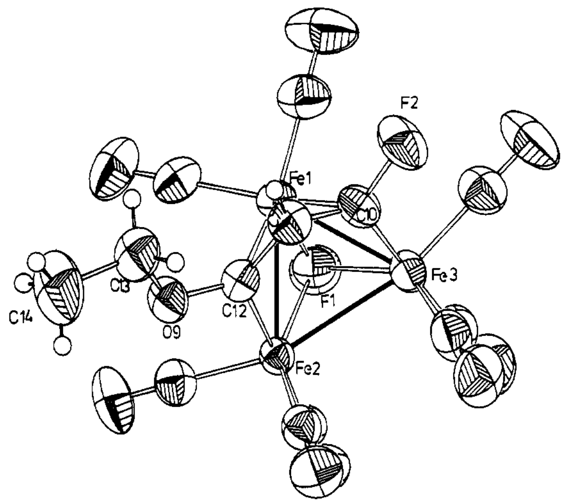

Figure 1. ORTEP plot of **3c**. Thermal ellipsoids are at 50% probability.

Discussion

Nonacarbonylbis(μ_3-fluoromethylidyne)triiron (**1**) reacts with various alkynes H–C≡C–R (**2a–f**) and H_3C–C≡C–R (**2g–l**) with carbon–carbon bond formation yielding diferra–allyl clusters (Scheme I). The ratio of the isomers was monitored by ^{19}F NMR spectroscopy, and in contrast to the reaction of $Fe_3(CO)_9(\mu_3\text{-}C\text{-}CH_3)(\mu_3\text{-}C\text{-}OC_2H_5)$ with alkynes[5] no ferrole type cluster has been observed among the products. Within the limits of the NMR sensitivity the hydrogen-substituted alkynes **2a–f** yield only one of the two possible isomers, whereas the methyl-substituted alkynes **2g–l** yield both isomers in a ratio depending on the size and

Table III. Spectroscopic Data for Compounds **3a–f**

IR,[a] cm^{-1}	^1H NMR,[b] ppm	^{19}F NMR,[c] ppm	^{13}C NMR,[b] ppm
$Fe_3(CO)_8(\mu_3\text{-}CF)(\mu_3\text{-}CF{-}CH{-}CCH_3)$ (**3a**)			
2088 (w), 2061 (w), 2042 (vs), 2028 (s), 2015 (w), 2005 (m)	3.02 ($\mathrm{CF{-}CH{-}CC}\mathit{H}_3$), 7.24 ($\mathrm{CF{-}C}\mathit{H}\mathrm{{-}CCH_3}$) ($^3J_{HF}$ = 9)	91.0 (μ_3-$\mathrm{C}\mathit{F}$), −5.2 ($\mathrm{C}\mathit{F}\mathrm{{-}CH{-}CCH_3}$) ($^3J_{HF}$ = 9)	37.3 ($\mathrm{CF{-}CH{-}C{-}}\mathit{C}\mathrm{H_3}$), 120.4 ($\mathrm{CF{-}}\mathit{C}\mathrm{H{-}C{-}CH_3}$) ($^2J_{CF}$ = 20), 204.4 and 207.3 (CO), 208.1 ($\mathrm{CF{-}CH{-}}\mathit{C}\mathrm{{-}CH_3}$) ($^3J_{CF}$ = 16), 241.6 ($\mathit{C}\mathrm{F{-}CH{-}C{-}CH_3}$) ($^1J_{CF}$ = 349), 333.2 (μ_3-CF) ($^1J_{CF}$ = 480)
$Fe_3(CO)_8(\mu_3\text{-}CF)(\mu_3\text{-}CF{-}CH{-}CC_6H_5)$ (**3b**)			
2087 (m), 2045 (s), 2029 (vs), 2008 (s), 2000 (m)	7.9 ($\mathrm{CF{-}CH{-}CC_6}\mathit{H}_5$)	92.1 (μ_3-$\mathrm{C}\mathit{F}$), −6.8 ($\mathrm{C}\mathit{F}\mathrm{{-}CH{-}CC_6H_5}$) ($^3J_{HF}$ = 9.8)	120.9 ($\mathrm{CF{-}}\mathit{C}\mathrm{H{-}C{-}C_6H_5}$) ($^2J_{CF}$ = 21), 207.2 ($\mathrm{CF{-}CH{-}}\mathit{C}\mathrm{{-}C_6H_5}$) ($^3J_{CF}$ = 5), 241.1 ($\mathit{C}\mathrm{F{-}CH{-}C{-}C_6H_5}$) ($^1J_{CF}$ = 348), 333.6 (μ_3-CF) $^1J_{CF}$ = 479), 127.6, 128.7, 129.0, and 151.1 (C_6H_5), 204.2 ($^3J_{CF}$ = 3) (CO), 207.8 (CO)
$Fe_3(CO)_8(\mu_3\text{-}CF)(\mu_3\text{-}CF{-}CH{-}COC_2H_5)$ (**3c**)			
2087 (w), 2046 (s), 2038 (vs), 2027 (s), 2011 (m), 1995 (w)	1.43 ($\mathrm{CF{-}CH{-}COCH_2C}\mathit{H}_3$) ($^3J_{HH}$ = 7.1), 3.99 ($\mathrm{CF{-}CH{-}COC}\mathit{H}_2\mathrm{CH_3}$), 4.29 ($\mathrm{CF{-}CH{-}COC}\mathit{H}_2\mathrm{CH_3}$) ($J_{ab}$ = −8.67), 7.01 ($\mathrm{CF{-}C}\mathit{H}\mathrm{{-}COCH_2CH_3}$) ($^3J_{HF}$ = 9.3)	86.7 (μ_3-CF), −9.4 ($\mathrm{C}\mathit{F}\mathrm{{-}CH{-}COCH_2CH_3}$) ($^3J_{HF}$ = 9.3)	100.7 ($\mathrm{CF{-}}\mathit{C}\mathrm{H{-}COCH_2CH_3}$) ($^2J_{CF}$ = 22), 232.7 ($\mathrm{CF{-}CH{-}}\mathit{C}\mathrm{OCH_2CH_3}$) ($^3J_{CF}$ = 17), 241.6 ($\mathit{C}\mathrm{F{-}CH{-}COCH_2CH_3}$) ($^1J_{CF}$ = 348), 333.6 (μ_3-CF) ($^1J_{CF}$ = 479), 205.6 ($^3J_{CF}$ = 4) (CO), 206.2 (CO), 70.8 ($\mathrm{CF{-}CH{-}CO}\mathit{C}\mathrm{H_2CH_3}$), 14.5 ($\mathrm{CF{-}CH{-}COCH_2}\mathit{C}\mathrm{H_3}$)
$Fe_3(CO)_8(\mu_3\text{-}CF)[\mu_3\text{-}CF{-}CH{-}CSi(CH_3)_3]$ (**3d**)			
2087 (m), 2041 (vs), 2029 (s), 2012 (m), 2000 (m)	0.47 [μ_3-$\mathrm{CF{-}CH{-}CSi(C}\mathit{H}_3)_3$], 7.7 [$\mu_3$-$\mathrm{CF{-}C}\mathit{H}\mathrm{{-}CSi(CH_3)_3}$] ($^3J_{HF}$ = 9.5)	92.1 (μ_3-CF), −2.2 [μ_3-$\mathrm{C}\mathit{F}\mathrm{{-}CH{-}CSi(CH_3)_3}$]	125.4 [μ_3-$\mathrm{CF{-}}\mathit{C}\mathrm{H{-}CSi(CH_3)_3}$] ($^2J_{CF}$ = 20, $^1J_{CH}$ = 164), 205.3 [μ_3-$\mathrm{CF{-}CH{-}}\mathit{C}\mathrm{Si(CH_3)_3}$] ($^3J_{CF}$ = 11), 241.5 [μ_3-$\mathit{C}\mathrm{F{-}CH{-}CSi\ (CH_3)_3}$] ($^1J_{CF}$ = 353), 334.5 (μ_3-CF) ($^1J_{CF}$ =479), 204.1 and 208.5 (CO), 206 (br, CO), 2.1 [μ_3-$\mathrm{CF{-}CH{-}CSi(}\mathit{C}\mathrm{H_3)_3}$] ($^1J_{CH}$ = 118.4)
$Fe_3(CO)_8(\mu_3\text{-}CF)(\mu_3\text{-}CF{-}CH{-}CCF_3)$ (**3e**)			
2097 (m), 2055 (vs), 2047 (m), 2038 (s), 2024 (m), 2019 (m)	7.86 ($\mathrm{CF{-}C}\mathit{H}\mathrm{{-}CCF_3}$) ($^3J_{HF}$ = 9.2)	100.9 (μ_3-$\mathrm{C}\mathit{F}$), −2.7 ($\mathrm{C}\mathit{F}\mathrm{{-}CH{-}CCF_3}$) ($^3J_{HF}$ = 9.2), −52.6 ($\mathrm{CF{-}CH{-}CC}\mathit{F}_3$)	120.8 ($\mathrm{CF{-}}\mathit{C}\mathrm{H{-}CCF_3}$) ($^3J_{CF}$ = 6, $^2J_{CF}$ = 24), 128.7 ($\mathrm{CF{-}CH{-}C}\mathit{C}\mathrm{F_3}$) ($^1J_{CF}$ = 276), 181.7 ($\mathrm{CF{-}CH{-}}\mathit{C}\mathrm{CF_3}$) ($^2J_{CF}$ = 33, $^3J_{CF}$ = 17), 239.3 ($\mathit{C}\mathrm{F{-}CH{-}CCF_3}$) ($^1J_{CF}$ = 349), 348.6 (μ_3-CF) ($^1J_{CF}$ = 482), 202.9 and 204.7 (CO), 206 (br, CO)
$Fe_3(CO)_8(\mu_3\text{-}CF)(\mu_3\text{-}CF{-}CH{-}CSF_5)$ (**3f**)			
2098 (vw), 2058 (vs), 2040 (s), 2028 (vw), 2003 (vw)	8.06 ($\mathrm{CF{-}C}\mathit{H}\mathrm{{-}CSF_5}$) ($^3J_{HF}$ = 9.7)	101.6 (μ_3-$\mathrm{C}\mathit{F}$), −4.3 ($\mathrm{C}\mathit{F}\mathrm{{-}CH{-}CSF_5}$), 87.1 ($\mathrm{CF{-}CH{-}CS}\mathit{F}_5$), 73.0 ($\mathrm{CF{-}CH{-}CS}\mathit{F}_5$) ($J_{AB}$ = 146)	124.6 ($\mathrm{CF{-}}\mathit{C}\mathrm{H{-}CSF_5}$) ($^2J_{CF}$ = 24, $^3J_{CF}$ = 7), 236.6 ($\mathrm{C}\mathit{F}\mathrm{{-}CH{-}CSF_5}$) ($^1J_{CF}$ = 350), 336.5 (μ_3-$\mathrm{C}\mathit{F}$) ($^1J_{CF}$ = 483), 206.3 and 204.5 (CO)

[a] Solution in *n*-hexane. [b] Solution in $CDCl_3$; $\delta(CHCl_3)$ = 7.24 ppm and $\delta(CDCl_3)$ = 77.1 ppm, respectively. *J* values are in Hz. [c] Solution in $CDCl_3$; $CFCl_3$ as external reference standard. *J* values are in Hz.

Table IV. Spectroscopic Data for Compounds **3g–l**

IR,[a] cm^{-1}	^{1}H NMR,[b] ppm	^{19}F NMR,[c] ppm	^{13}C NMR,[b] ppm
Fe$_3$(CO)$_8$(μ_3-CF)[μ_3-CF–C(CH$_3$)–CC$_2$H$_5$] (**3(I)g**)			
2085 (w), 2039 (vs), 2025 (s), 2001 (m)	1.67 [CF–C(CH$_3$)–CCH$_2$C*H*$_3$] ($^3J_{HH}$ = 7.6), 2.38 [CF–C(C*H*$_3$)–CCH$_2$CH$_3$] ($^4J_{HF}$ = 3), 3.36–3.58 [CF–C(CH$_3$)–CC*H*$_2$CH$_3$] (abx$_3$ pattern)	–0.8 [C*F*–C(CH$_3$)–CCH$_2$CH$_3$] ($^4J_{HF}$ = 3), 84.4 (μ_3-CF)	
Fe$_3$(CO)$_8$(μ_3-CF)[μ_3-CF–C(C$_2$H$_5$)–CCH$_3$] (**3(II)g**)			
	1.15 [CF–C(CH$_2$C*H*$_3$)–CCH$_3$] ($^3J_{HH}$ = 7.6), 3.06 [CF–C(CH$_2$CH$_3$)–CC*H*$_3$], 2.54–2.83 [CF–C(C*H*$_2$CH$_3$)–CCH$_3$] ($^4J_{HF}$ = 3)	–3.1 [CF–C(CH$_2$CH$_3$)–CCH$_3$] ($^4J_{HF}$ = 3), 90.4 (μ_3-C*F*)	
Fe$_3$(CO)$_8$(μ_3-CF)[μ_3-CF–C(CH$_3$)–CCH(CH$_3$)$_2$] (**3(I)h**)			
2084 (s), 2061 (m), 2038 (vs), 2024 (vs), 2009 (s), 2000 (s), 1979 (m)	1.54 [CF–C(CH$_3$)–CCH(C*H*$_3$)$_2$] ($^3J_{HH}$ = 6.7), 1.65 [CF–C(CH$_3$)–CCH(C*H*$_3$)$_2$] ($^3J_{HH}$ = 7.1), 2.34 [CF–C(C*H*$_3$)–CCH(CH$_3$)$_2$] ($^4J_{HF}$ = 3.6), 3.54 [CF–C(CH$_3$)–CC*H*(CH$_3$)$_2$] ($^3J_{HH}$ ≈ 7)	89.1 (μ_3-C*F*), 4.7 [C*F*–C(CH$_3$)–CCH(CH$_3$)$_2$] ($^4J_{HF}$ = 3.6)	
Fe$_3$(CO)$_8$(μ_3-CF)[μ_3-CF–C(C$_3$H$_7$)–CCH$_3$] (**3(II)h**)			
	1.09 [CF–C{CH(C*H*$_3$)$_2$}–CCH$_3$] ($^3J_{HH}$ = 7.2), 2.94 [CF–C{CH(CH$_3$)$_2$}–CC*H*$_3$], 3.09 [CF–C{C*H*(CH$_3$)$_2$}–CCH$_3$]	90.6 (μ_3-C*F*), 3.6 [C*F*–C{CH(CH$_3$)$_2$}–CCH$_3$]	
Fe$_3$(CO)$_8$(μ_3-CF)[μ_3-CF–C(CH$_3$)–COC$_2$H$_5$] (**3(I)i**)			
2086 (m), 2080 (m), 2042 (vs), 2033 (s), 2024 (s), 2012 (s), 2005 (s)	1.62 [CF–C(CH$_3$)–COCH$_2$C*H*$_3$] ($^3J_{HH}$ = 7.0), 2.31 [CF–C(C*H*$_3$)–COCH$_2$CH$_3$] ($^4J_{HF}$ = 2.5), 4.18 [CF–C(CH$_3$)–COC*H*$_2$CH$_3$], 4.33 [CF–C(CH$_3$)–COC*H*$_2$CH$_3$] ($^2J_{ab}$ = –15.9)	87.2 (μ_3-C*F*) (J_{FF} = 1.2), –10.7 [C*F*–C(CH$_3$)–COCH$_2$CH$_3$] ($^4H_{HF}$ = 2.4)	124.4 [CF–*C*(CH$_3$)–COCH$_2$CH$_3$] ($^2J_{CF}$ = 14.6), 235.1 [CF–C(CH$_3$)–*C*OCH$_2$CH$_3$] ($^3J_{CF}$ = 15.9), 236.4 [*C*F–C(CH$_3$)–COCH$_2$CH$_3$] ($^1J_{CF}$ = 349), 334.0 (μ_3-CF) ($^1J_{CF}$ = 479), 205.2 and 206.0 (CO), 15.1 and 15.3 [CF–C(*C*H$_3$)–COCH$_2$*C*H$_3$], 73.1 [CF–C(CH$_3$)–CO*C*H$_2$CH$_3$]
Fe$_3$(CO)$_8$(μ_3-CF)[μ_3-CF–C(OC$_2$H$_5$)–CCH$_3$] (**3(II)i**)			
		92.5 (μ_3-CF), –22.1 [C*F*–C(OC$_2$H$_5$)–CCH$_3$]	
Fe$_3$(CO)$_8$(μ_3-CF)[μ_3-CF–C(CH$_3$)–CC$_6$H$_5$] (**3(I)k**)			
2085 (m), 2043 (vs), 2038 (vs), 2027 (s), 2011 (w), 2005 (w), 1994 (w)	2.52 [CF–C(C*H*$_3$)–CC$_6$H$_5$] ($^4J_{HF}$ = 3.4), 7.71 [CF–C(CH$_3$)–CC$_6$H$_5$]	91.3 (μ_3-CF), –1.5 [C*F*–C(CH$_3$)–CC$_6$H$_5$] ($^4J_{HF}$ = 3.4)	18.5 [CF–C(*C*H$_3$)–CC$_6$H$_5$] ($^3J_{CF}$ = 5), 127.4, 127.9, 128.4 and 150.5 [CF–C(CH$_3$)–C*C*$_6$H$_5$], 132.4 [CF–*C*(CH$_3$)–CC$_6$H$_5$] ($^2J_{CF}$ = 13), 206.5 [CF–C(CH$_3$)–*C*C$_6$H$_5$] ($^3J_{CF}$ = 15), 204.0 and 208.6 (*C*O), 237.5 [*C*F–C(CH$_3$)–CC$_6$H$_5$] ($^1J_{CF}$ = 352), 337.7 (μ_3-CF) ($^1J_{CF}$ = 479)
Fe$_3$(CO)$_8$(μ_3-CF)[μ_3-CF–C(COOCH$_3$)–CCH$_3$] (**3(II)l**)			
2098 (w), 2045 (vs), 2030 (m), 2009 (w)	2.9, 3.9	93.4, –7.4	34.9 [CF–C(COOCH$_3$)–C*C*H$_3$], 53.5 [CF–C(COO*C*H$_3$)–CCH$_3$], 128.7 [CF–*C*(COOCH$_3$)–CCH$_3$] ($^2J_{CF}$ = 17), 164.4 [CF–C(*C*OOCH$_3$)–CCH$_3$], 198.6 and 206.2 (CO), 202.3 [CF–C(COOCH$_3$)–*C*CH$_3$] ($^3J_{CF}$ = 11), 235.1 [*C*F–C(COOCH$_3$)–CCH$_3$] ($^1J_{CF}$ = 353), 333.8 (μ_3-CF) ($^1J_{CF}$ = 481)

[a] Solution in *n*-hexane. [b] Solution in CDCl$_3$; δ(CHCl$_3$) = 7.24 ppm and δ(CDCl$_3$) = 77.1 ppm, respectively. *J* values are in Hz. [c] Solution in CDCl$_3$; CFCl$_3$ as external reference standard. *J* values are in Hz.

electronic effects of substituent R (Scheme I).

According to the NMR spectroscopic data (Table III) the carbon–carbon bond formation has occurred at the sterically less hindered site at the CH carbon atom. All of these diferra–allyl clusters **3a–f** exhibit two signals in the ^{19}F NMR spectra, one low-field signal, which is due to the fluorine atom of the fluoromethylidyne group, and a signal around zero ppm, which belongs to the diferra-allyl moiety. This high-field signal exhibits a ^3J fluorine–hydrogen coupling constant of 9–10 Hz, proving that the fluorine and hydrogen atoms are in a vicinal position. The coupling constant between the two fluorine atoms is very small (<1.5 Hz) and has been observed only in a few cases. The ^{1}H NMR spectra of **3a–f** exhibit the resonance of the CH group as a doublet between 7.5 and 8.5 ppm besides the resonances of the organic moiety. As the clusters **3a–f** are chiral, the protons of the methylene group of **3c** are diastereotropic and an ABC$_3$ pattern was observed for the OC$_2$H$_5$ group. The ^{13}C{^{1}H} NMR spectra of all of these compounds show a very low field resonance between 330 and 350 ppm with a very large carbon fluorine coupling constant of about 480 Hz, indicating the presence of a μ_3-fluoromethylidyne ligand. One of the two further low field signals between 200 and 250 ppm, which can be assigned to the terminal carbon atoms of the allyl moiety, possesses a large carbon–fluorine coupling constant of about 350 Hz, whereas the other one shows only a small carbon–fluorine coupling. The resonance of the central carbon atom of the allyl moiety is observed around 120 ppm with a CF coupling constant between 15 and 25 Hz. The carbonyl carbon atoms of the Fe(CO)$_2$ fragment give sharp signals, whereas the resonances of the Fe(CO)$_3$ fragments are observed only as broad resonances at ambient temperature due to rapid exchange processes.

In the reaction of Fe$_3$(CO)$_9$(μ_3-CF)$_2$ (**1**) with the methyl-substituted alkynes **2g–l**, however, the ratio of the isomers **3(I)g–l** and **3(II)g–l** depends on the size and the electronic effects of the

Table V. Selected Interatomic Distances (Å) and Angles (deg) of **3c** with Estimated Standard Deviations in Parentheses

Distances			
Fe1–Fe2	2.505 (1)	Fe3–C10	1.959 (5)
Fe1–Fe3	2.502 (2)	C9–F1	1.353 (5)
Fe1–C9	1.767 (5)	C10–C11	1.385 (6)
Fe1–C10	2.022 (5)	C10–F2	1.370 (5)
Fe1–C11	2.174 (5)	C11–C12	1.410 (7)
Fe1–C12	2.078 (4)	C11–H1	0.94 (5)
Fe2–Fe3	2.601 (1)	C12–O9	1.351 (5)
Fe2–C9	1.985 (4)	C13–C14	1.48 (1)
Fe2–C12	2.015 (5)	C13–O9	1.445 (7)
Fe3–C9	2.000 (5)		
Angles			
Fe2–Fe1–Fe3	62.59 (4)	Fe2–C9–Fe3	81.5 (2)
Fe2–Fe1–C10	86.8 (2)	Fe2–C9–F1	127.0 (3)
Fe2–Fe1–C11	80.2 (2)	Fe3–C9–F1	127.2 (3)
Fe2–Fe1–C12	51.1 (2)	Fe1–C10–Fe3	77.9 (2)
Fe3–Fe1–C10	49.9 (2)	Fe1–C10–C11	76.8 (3)
Fe3–Fe1–C11	80.1 (2)	Fe1–C10–F2	127.9 (3)
Fe3–Fe1–C12	88.5 (2)	Fe3–C10–C11	128.1 (4)
C10–Fe1–C11	38.3 (2)	Fe3–C10–F2	118.2 (3)
C10–Fe1–C12	69.9 (2)	C11–C10–F2	113.2 (4)
C11–Fe1–C12	38.6 (2)	Fe1–C11–C10	64.9 (3)
Fe1–Fe2–Fe3	58.65 (3)	Fe1–C11–C12	67.0 (3)
Fe1–Fe2–C12	53.4 (2)	Fe1–C11–H1	130 (3)
Fe3–Fe2–C12	87.2 (2)	C10–C11–C12	114.4 (4)
C9–Fe2–C12	97.8 (2)	C10–C11–H1	121 (3)
Fe1–Fe3–Fe2	58.77 (3)	C12–C11–H1	123 (3)
Fe1–Fe3–C10	52.2 (2)	Fe1–C12–Fe2	75.4 (2)
Fe2–Fe3–C9	49.0 (2)	Fe1–C12–C11	74.3 (3)
Fe2–Fe3–C10	85.5 (2)	Fe1–C12–O9	131.4 (3)
C9–Fe3–C10	96.4 (2)	Fe2–C12–C11	123.0 (3)
Fe1–C9–Fe2	83.5 (2)	Fe2–C12–O9	113.9 (3)
Fe1–C9–Fe3	83.0 (2)	C11–C12–O9	122.5 (4)
Fe1–C9–F1	136.2 (3)		

substituent R. In accordance with the above discussion of the NMR spectroscopic data (Tables III and IV) of **3a–f**, both isomers **3(I)g–l** and **3(II)g–l** possess a diferra–allyl structure (Scheme I).

On the basis of the ^1H NMR spectra of the compounds **3(I)g–l** and **3(II)g–l** (Table IV), the major isomers **3(I)g–k** and **3(II)l** were formed. The ^1H NMR spectra of the isomers I, which have the methyl substituent in the position vicinal to the fluorine substituent, exhibit a splitting of the resonances of the methyl protons into a doublett due to coupling to ^{19}F with $^4J_{HF} \approx 2$–4 Hz. In addition, these resonances are generally observed at higher field than the resonances of the methyl protons of isomer II.

For the substituents R = C_2H_5 and i-C_3H_7, which are only slightly larger than the methyl substituent, only a small preference of the isomers **3(I)g** and **3(I)h** versus **3(II)g** and **3(II)h** is observed. In addition, the ethyl and ispropyl group have the same electronic effect as that of the methyl group. With substituents on the alkyne with a –I and +M effect (R = OC_2H_5, C_6H_5), for **2i–k** the formation of the isomer I is highly favored. With the ethoxy group, a **3(I)i**:**3(II)i** ratio of 9:1 is observed. The phenyl substituent results in the formation of only the isomer **3(I)k** within the limits of sensitivity of ^{19}F NMR spectroscopy.

Surprisingly the reaction of **1** with the alkyne $H_3C\text{–}C{\equiv}C\text{–}COOCH_3$ (**2l**) yields only the isomer **3(II)l**, as can be seen by the missing coupling of the methyl protons to the fluorine substituent and the low-field resonance of these protons. In addition the ^{13}C resonance of the methyl carbon atom is shifted to 34.9 ppm compared to 15.1 and 18.5 ppm for **3(I)i** and **3(I)k**. These results may be rationalized as follows: The carboethoxy group possesses a –I and –M effect, whereas both the phenyl and ethoxy substituents have –I and +M effects. Thus, the different sides of alkylidyne–alkyne coupling with the methyl-substituted derivatives can be a result of the electronic effects of the substituents. However, further investigations of the electronic effects on the regioselectivity of this carbon–carbon bond formation reaction are necessary. However, the reaction of the alkynes $H\text{–}C{\equiv}C\text{–}R$ (**2a–f**) is strictly regioselective, resulting in only the isomer I independent of the electronic effects of the substituents. Thus, the regioselectivity of the alkylidyne–alkyne coupling reaction of **1** is much more distinct than the reaction of $Ru_3(H)_3(CO)_9(\mu_3\text{-}CX)$, which even for the hydrogen-substituted alkynes $HC{\equiv}CR$ (R = Ph, n-Bu, t-Bu, CO_2Me) results in mixtures of the two isomers.[16a] In addition 1,3-dimetalla-substituted allyls are *not* products from the reaction of $Co_3(CO)_9(\mu_3\text{-}CX)$ clusters with alkynes.[28] None of these clusters **3a–l** show any tendency at ambient temperature to undergo isomerization to the corresponding ferrole clusters, which have been obtained by Mathieu et al. on the thermal reaction of $Fe_3(CO)_9(\mu_3\text{-}CCH_3)(\mu_3\text{-}C\text{-}OC_2H_5)$[5] with alkynes. However, whereas $Fe_3(CO)_9(\mu_3\text{-}CF)(\mu_3\text{-}CF\text{–}CPh\text{–}CPh)$ can be prepared both thermally and photochemically,[11] $Fe_3(CO)_9(\mu_3\text{-}CF)(\mu_3\text{-}CF\text{–}CCH_3\text{–}CCH_3)$ decomposes at 100 °C, forming three products[29] including at least one ferrole type cluster.

Structure of $Fe_3(CO)_8(\mu_3\text{-}CF)(\mu_3\text{-}CF\text{–}CH\text{–}C\text{–}OC_2H_5)$ (3c). In accordance with spectroscopic data, the results of the X-ray crystal structure determination of $Fe_3(CO)_8(\mu_3\text{-}CF)(\mu_3\text{-}CF\text{–}CH\text{–}C\text{-}OC_2H_5)$ (**3c**) (Figure 1, Tables I, II, and V) demonstrate that the carbon–carbon bond formation has occurred at the sterically less hindered side of the alkyne.

The molecule $Fe_3(CO)_8(\mu_3\text{-}CF)(\mu_3\text{-}CF\text{–}CH\text{–}C\text{–}OC_2H_5)$ (**3c**) consists of a isosceles iron triangle, which is capped by one fluoromethylidyne group. The two iron–iron bonds (Fe1–Fe2, Fe1–Fe3), which are bridged by the allyl moiety, are about 10 pm shorter than the other iron–iron bond (Fe2–Fe3). In addition, the distance of the unique iron atom Fe1 to the apical carbon atom C9 (176.7 (5) pm) is significantly shorter than those to the remaining iron atoms Fe2 and Fe3 (Fe2–C9 = 198.5 (4) pm, Fe3–C9 = 200.0 (5) pm), which are very similar. The terminal carbon atoms of the C_3 moiety, C10 and C12, show similar distances to the iron atoms Fe1, Fe3 and Fe1, Fe2, respectively, in a range from 195.9 (5) to 207.8 (5) pm. The central atom of the C_3 moiety is bonded only to the iron atom Fe1 with a relatively long distance of 217.4 (5) pm. According to the bond lengths and angles, the $Fe3\text{–}CF\text{–}CH\text{–}C(OC_2H_5)\text{–}Fe2$ moiety can be regarded as a 1,3-diferra-substituted allyl ligand, which is coordinated to the iron atom Fe1. In an alternative description the atoms Fe2, Fe3, C10, C11, C12, and Fe1 form a pentagonal nido cluster, which is capped by a fluoromethylidyne group. This description is in accord with Wade's rules,[30] although the cluster possesses the less common capped nido structure. The ferrole type clusters of Mathieu et al.[5] can be regarded as isomeric closo clusters.

Acknowledgment. This research was supported by the Deutsche Forschungsgemeinschaft and the Fonds der Chemischen Industrie. We acknowledge Prof. Dr. J. Fuchs for his assistance in the crystallographic work.

Supplementary Material Available: For **3c**, tables listing full crystallographic data, positional and thermal parameters, and interatomic distances and angles (5 pages); listings of observed and calculated structure factors (20 pages). Ordering information is given on any current masthead page.

---

(28) Dickson, R. S.; Tailby, G. R. *Aust. J. Chem.* **1970**, *23*, 229.
(29) Lentz, D.; Michael-Schulz, H. Unpublished results.
(30) Wade, K. *Adv. Inorg. Chem. Radiochem.* **1976**, *18*, 1.